A Letters Journal Exploring the Frontiers of Physics

June 2010

EPL, **90** (2010) 64001
doi: 10.1209/0295-5075/90/64001

www.epljournal.org

Smectic rheology close to the smectic-nematic transition

S. Fujii[1(a)], Y. Ishii[2], S. Komura[3] and C.-Y. D. Lu[4]

[1] *Department of Chemistry, Nagaoka University of Technology - Niigata 940-2188, Japan*
[2] *Department of Physics and Applied Physics, Waseda University - Tokyo 169-8555, Japan*
[3] *Department of Chemistry, Graduate School of Science and Engineering, Tokyo Metropolitan University Tokyo 192-0397, Japan*
[4] *Department of Chemistry, National Taiwan University - Taipei 106, Taiwan*

received 10 February 2010; accepted in final form 15 June 2010
published online 30 June 2010

PACS 47.57.Qk – Complex fluids and colloidal systems: Rheological aspects
PACS 64.70.mj – Experimental studies of liquid crystal transitions
PACS 61.30.Jf – Defects in liquid crystals

Abstract – We study the rheological properties of a thermotropic liquid crystal, 8CB, in the smectic phase close to the smectic-nematic (Sm-N) transition temperature. Three different regimes were identified in the flow curves at different temperatures: i) appearance of the yield stress at low stresses, ii) power law behavior at intermediate shear stresses, and iii) Newtonian at higher shear stresses. The vanishing of the yield stress at the Sm-N transition temperature is correlated with a rapid growth of focal conic domains. The constructed dynamic phase diagram exhibits the two different smectic phases together with the flow-induced Sm-N transition.

Introduction. – The rheology of smectic liquid crystals is a long-standing puzzle [1–3]. Although the theory predicts a liquid response when the smectic layers are aligned parallel to the shear plane, some experiments showed that the system behaves as a solid until a critical shear stress is exceeded [4–6]. This means that even the oriented smectic liquid crystal behaves as a yield stress fluid [7] at very low stress. Such a peculiar behavior can be attributed to the presence of defects such as focal conic domains in the smectic layers, because they will act to hinder layer sliding in the low stress limit. Indeed it was seen that the focal conic domain density strongly correlates with the viscosity [4]. At stress levels slightly above the yield stress, there is a yielding regime and the smectic phase starts to flow [5,6]. In general, the yield stress of a stationary sample fluctuates considerably and can be highly dependent on its flow history such as a sample loading process. Meyer *et al.* proposed a theory of smectic rheology which is explicitly based on the screw defect line motion [8,9]. By using the Orowan relation [10], they obtained a power law behavior of the constitutive relation between the shear rate $\dot{\gamma}$ and the shear stress σ such that $\dot{\gamma} \sim \sigma^m$ with a universal exponent $m = 5/3$. This shear thinning ($m > 1$) behavior was confirmed not only for a thermotropic smectic liquid crystal, but also in the lamellar phases of a copolymer solution and a lyotropic system [8,9]. Later a slightly different exponent $m = 3/2$ was predicted by some of the present authors who considered the motion of dislocation loops under shear flow which causes the continuous production of dislocations [11].

On the other hand, the proliferation of dislocations takes place close to the smectic-nematic (Sm-N) transition point even in the absence of any applied external field, *i.e*, in thermal equilibrium. This is known as the dislocation-loop-mediated smectic melting or the dislocation unbinding transition proposed by Helfrich in 1978 [12] and further developed by other scientists [13]. For smectic systems, the unbinding of the dislocation loop is described as the divergence of the defect size. Recently, the appearance of dislocation loops was directly observed using freeze-fracture transmission electron microscopy in a lyotropic system in the vicinity of the smectic-cholesteric (chiral nematic) transition [14]. Although the concept of topological melting is quite important in many condensed-matter systems, its experimental evidence is very limited. Especially, it is totally unknown how the unbinding of dislocation loops affects the average size of focal conic domains which play an important role in the smectic rheology. The aim of the present letter is to investigate the rheological properties of a thermotropic liquid crystal (8CB) in the smectic phase close to the Sm-N transition temperature. This is an

(a) E-mail: sfujii@mst.nagaokaut.ac.jp

interesting situation because the proliferation of dislocation loops is induced by both equilibrium thermal fluctuations and non-equilibrium shear flow. One can naturally expect that the effects of temperature and flow are strongly correlated so that a very unique rheological response could be observed as the transition is approached from below. Our rheology measurement reveals that the Sm-N transition temperature is lowered in the presence of an applied shear stress. We also address the issue of the universal shear thinning exponent m in the smectic phase far from the transition point as well as the flow-induced orientation transition. To our knowledge, the present work is the first systematic study on the smectic rheology over wide shear stress and temperature ranges.

Before explaining our results, we briefly refer to some of the additional related works. As the N-Sm transition is approached from above in the nematic phase under shear flow, Safinya *et al.* showed that one of the viscosities diverges due to the critical slowing-down of the smectic order-parameter fluctuations [15,16]. When the temperature of the smectic phase is not very close to the transition point, Panizza *et al.* performed X-ray scattering studies under shear flow [17]. They found that a discontinuous dynamic transition separates between the two smectic orientations exhibiting different rheological behaviors; the system is shear thinning ($m = 2$) at low shear rates, while it becomes Newtonian ($m = 1$) at high shear rates. More recently, the frequency-dependent shear modulus of the smectic liquid crystal in a colloidal aerosil gel was analyzed [18] using the concept of soft glassy rheology [19]. For a lyotropic lamellar phase, on the other hand, it was also shown that the proliferation of dislocation strongly affects the rheological and orientational properties [20,21].

Experimental. – We used the thermotropic liquid-crystal 4-*n*-octyl-4′-cyanobiphenyl (8CB) as a smectic liquid crystal in this study. The phase behavior and some physical properties of 8CB have been studied in the literatures [15,17]. 8CB was obtained from SYNTHON Chemicals GmbH & Co., Germany and was used without further purification. Rheological measurements were performed using the stress-controlled rheometer, Anton Paar MCR-300, equipped with a cone-plate shear cell which has a diameter of 50 mm and a cone angle of 1 degree. In contrast to ref. [4], no surface treatment has been done in our experiment. The lack of the homeotropic alignment of smectic layers may easily induce the nucleation of focal parabolae under shear flow. Temperature was controlled within 0.02 K by a Peltier device attached to the rheometer. We determined the smectic-A–to–nematic transition temperature $T_{\rm SN}$ by the dynamic viscoelastic measurement. From the condition that the storage modulus disappears, we obtained $T_{\rm SN} = 33.4\,^{\circ}$C. This value is in good agreement with that reported previously [15]. In the rheological measurement, the shear stress was imposed and the shear rate was measured. The subsequent stress sweep proceeded from high to low stresses. Thus the samples were always pre-sheared before the measurement at every shear stress such that the defect density is well defined. Each shear stress was applied for 1000 s because the steady state was achieved within 600 s. The steady-state shear rate was averaged over 600–1000 s at every fixed shear stress. We also measured the temperature dependence of the shear viscosity under different applied shear stresses. Here the temperature was swept with the heating rate of 0.05 K/min from low to high values.

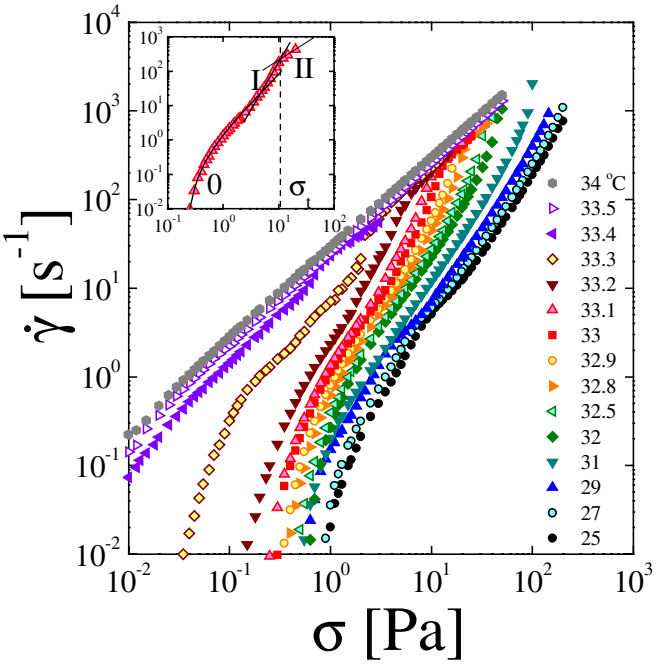

Fig. 1: (Colour on-line) Steady-state shear rate $\dot{\gamma}$ as a function of the applied shear stress σ at different temperatures. The inset shows a typical curve ($T = 33.1\,^{\circ}$C) divided into three regimes. Regime 0 is fitted by the Herschel-Bulkely model, eq. (1); Regime I is fitted by the power law behavior, eq. (2); and Regime II corresponds to the Newtonian behavior. $\sigma_{\rm t}$ indicates a stress where the transition from Regime I to Regime II takes place.

Microscope observation under shear flow was performed by using a Linkam CSS 450 shear cell which has a plate-plate shear geometry attached onto a Olympus microscope, BX-50, between crossed polarizers. The gap size between the two plates was fixed to 150 μm.

Results and discussion. –

Flow curves. Figure 1 shows the applied shear stress σ-dependence of the steady-state shear rate $\dot{\gamma}$ measured at different temperatures ranging from 25 to 34 °C (the latter being slightly above $T_{\rm SN} = 33.4\,^{\circ}$C). We first note that the slope of these flow curves was larger than unity for all the temperatures in the smectic phase, indicating a shear thinning behavior. However, these data cannot be expressed by a single power law behavior with a universal exponent m. Especially, the flow curves in the smectic phase exhibited non-zero shear stress, or the yield stress $\sigma_{\rm y}$, in the limit of $\dot{\gamma} \to 0$. As we shall describe below

in more detail, the whole behavior can be described by a combination of three different regimes. When the temperature is increased toward $T_{\rm SN}$, the curve shifted to lower shear stresses. Above $T_{\rm SN}$ in the nematic phase, only the Newtonian behavior with a single slope $m = 1$ could be found. An interesting behavior observed at higher temperatures within the smectic phase is the rheological transition from the shear thinning to the Newtonian behavior at higher shear stresses. The threshold shear stress for this rheological transition, denoted by $\sigma_{\rm t}$, shifted to lower stresses as the temperature was increased. A similar dynamic transition was reported in refs. [15,17] in which the authors attributed it to the shear-induced orientational transition of the smectic layers [22] from leek to perpendicular alignment. We also note that the steady shear data for 8CB at 26 °C in refs. [5,6] are in agreement with those in fig. 1.

Following the argument in ref. [6], the flow curves in the smectic phase were divided into three regimes; shear thinning with the yield stress at low stresses (Regime 0), shear thinning at intermediate shear stresses (Regime I), and Newtonian at higher shear stresses (Regime II). Note that $\sigma_{\rm t}$ separates between the Regimes I and II. A representative flow curve for $T = 33.1$ °C is shown in the inset of fig. 1. In order to quantify the yield stress in Regime 0, the data were fitted with the Herschel-Bulkely (HB) model describing a pseudo viscoplastic behavior

$$\sigma = \sigma_{\rm y} + A\dot{\gamma}^n, \tag{1}$$

where $\sigma_{\rm y}$ is the yield stress, A and n are adjustable parameters [7]. The best fit to the HB model is shown in the inset. In the intermediate Regime I, the data were fitted with a power law behavior as described in the introduction [6,8,9];

$$\sigma = C\dot{\gamma}^{1/m}, \tag{2}$$

where C is a pre-factor. This equation can be considered as the special case of eq. (1) be setting $\sigma_{\rm y} = 0$ and $n = 1/m$. In Regime II, the smectic phase becomes Newtonian with $m = 1$. All the other flow curves could be also well fitted by the HB model (Regime 0) and the power law separately (Regime I), although Regime II was not observed when the temperature is low.

The temperature dependence of $\sigma_{\rm y}$, A, n (Regime 0), C, m (Regime I) obtained by the best fit to eqs. (1) and (2), respectively, are summarized in fig. 2. We see that $\sigma_{\rm y}$ and A showed a remarkable temperature dependence especially in the vicinity of the Sm-N transition, while the exponent n depends only weakly on temperature. Notice that both $\sigma_{\rm y}$ and A vanish at $T = T_{\rm SN}$, and the values of n are always less than unity. On the other hand, both C and m were almost constant up to 32 °C, but increased remarkably in the vicinity of the Sm-N transition. The increase in m implies that the degree of shear thinning is more enhanced close to the transition. The constant value of $m \approx 1.7$ at low temperatures is almost consistent with the experimental result $m = 1.67$ and the theoretical

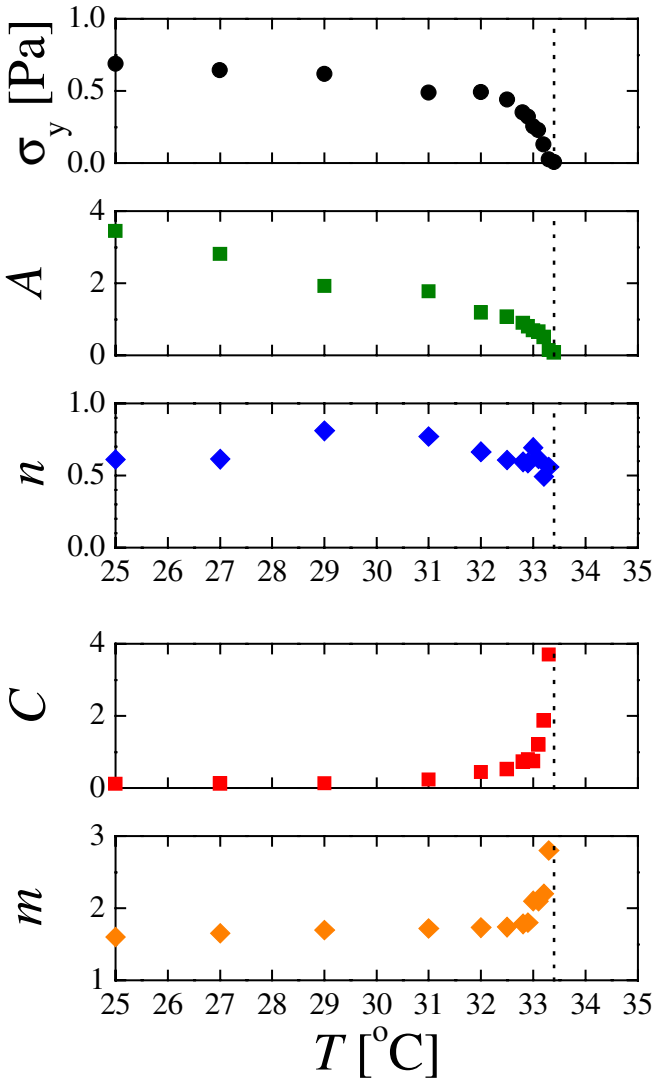

Fig. 2: (Colour on-line) The yield stress $\sigma_{\rm y}$, the pre-factor A, and the exponent n in eq. (1), the pre-factor C and the shear thinning exponent m in eq. (2) as a function of the temperature. These values are obtained by the best fit in fig. 1 for each regime. Vertical dotted line indicates the Sm-N transition temperature; $T_{\rm SN} = 33.4$ °C.

prediction $m = 5/3$ in refs. [8,9]. A slightly larger exponent $m = 2$ was reported for 8CB at 31 °C [17]. It should be noted, however, that the determination of m includes some arbitrariness depending on how we identify the range of each regime. The constant viscosity measured in Regime II was about 0.045 Pa s. This value is in reasonable agreement with the previously obtained value 0.036 Pa s [17]. We also note that it is close to the viscosity value measured in the nematic phase.

In ref. [4], Horn and Kleman reported that 8CB behaves as a Bingham fluid at 25 °C, *i.e.*, $A = \eta_{\rm app}$ and $n = 1$ ($\eta_{\rm app}$ is the apparent viscosity). Such a different exponent can be attributed to the imposed homeotropic alignment of the smectic sample in their measurement. In our experiment, the imperfect alignment of the homeotropic anchoring may

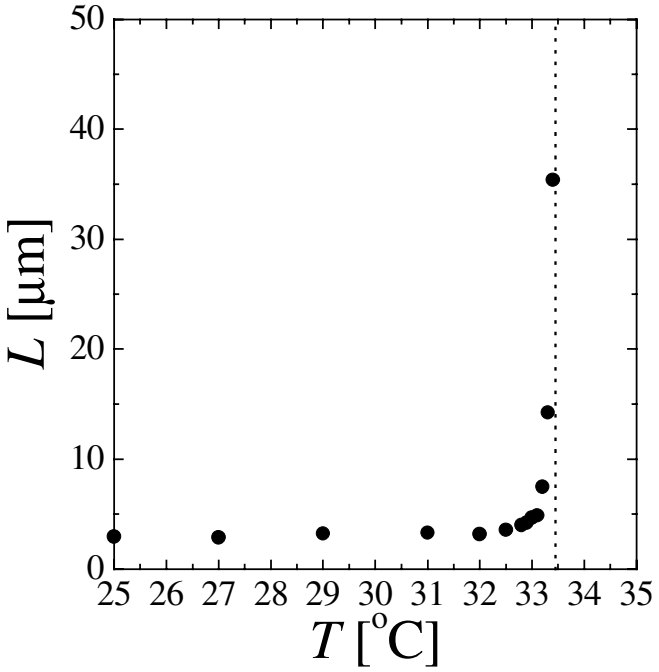

Fig. 3: The size of focal domains L as a function of the temperature. We have used eq. (3), and the curvature elastic constant K is taken to be constant over the temperature range performed in this study. The vertical dotted line indicates $T = T_{\rm SN}$.

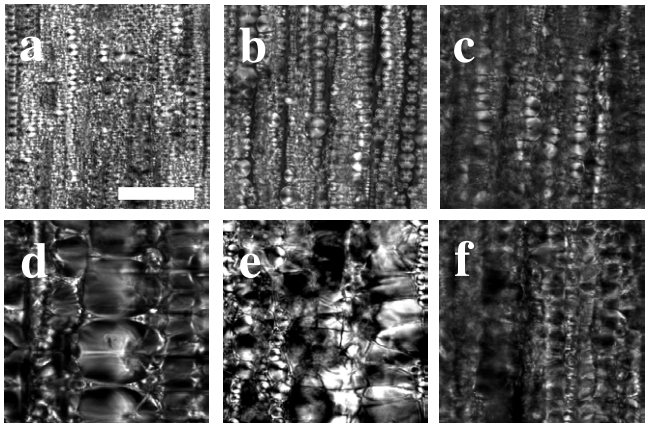

Fig. 4: Top: polarized microscopic images at a shear rate of $\dot\gamma = 1\,{\rm s}^{-1}$ for (a) $T = 25\,^\circ$C, (b) $29\,^\circ$C and (c) $31\,^\circ$C, respectively. Bottom: polarized microscopic images at $33\,^\circ$C under a shear of (d) $\dot\gamma = 0.1\,{\rm s}^{-1}$, (e) $1\,{\rm s}^{-1}$ and (f) $10\,{\rm s}^{-1}$, respectively. Flow is applied along the longitudinal direction. The scale bar corresponds to $100\,\mu$m.

enhance the nucleation of focal conic domains under shear flow. It should be stressed, however, that the obtained flow curves in fig. 1 are completely reproducible even without any surface treatment.

We note that the Newtonian behavior of Regime II in fig. 1 has nothing to do with the Newtonian behavior in Regime II discussed in ref. [6]. In the latter case, viscosity is independent of shear rate only because molecular motion keeps the molecular configuration undisturbed by the flow if $\dot\gamma R^2/D < 1$, where R is the molecular size and D is the diffusion coefficient. In the present case, the smectic becomes Newtonian when the layers align perpendicular to the shear flow, as we will discuss later. Hence the constant viscosity 0.045 Pa s obtained in Regime II corresponds to η_2, *i.e.*, the shear viscosity in the plane of the layers [2].

Focal conic domain size. For stresses lower than $\sigma_{\rm y}$, our view is that smectic behaves as an elastic solid with a modulus determined by the defect size. Above the yield stress, on the other hand, the motion of defects would dominate the rheological properties. According to Horn and Kleman [2,4], the yield stress was related to the focal conic domain size L by a dimensional analysis as follows:

$$\sigma_{\rm y} \approx \frac{K}{L^2}. \tag{3}$$

Here, K is the curvature elastic modulus [23]. Since K is known to be almost constant around the transition temperature with the value $K = (5.2 \pm 0.3) \times 10^{-12}$ N [24], we are able to extract the temperature dependence of L as shown in fig. 3. Here we see a remarkable growth of the focal conic domain size L as $T_{\rm SN}$ is approached from below.

Figure 4 shows the polarized microscopic images observed at different temperatures and different applied shear rates. Along the flow direction, oily streaks are formed due to the stacking of focal conic domains. A similar texture under flow was shown in fig. 5 of ref. [9]. When comparing between figs. 4(a)–(c) and (e) at fixed shear rate $\dot\gamma = 1\,{\rm s}^{-1}$, we observe that the width of the oily streak becomes larger as the temperature is increased towards $T_{\rm SN}$. The size of the focal conic domain is almost in accord with the estimated size L in fig. 3. Hence it is reasonable to consider that the vanishing of $\sigma_{\rm y}$ at $T_{\rm SN}$ in fig. 2 is closely related to the rapid growth of L as shown in figs. 3 and 4. The present result is an indication of the dislocation unbinding behavior, because the growth of the focal conic domains close to the transition point may be caused by the increment of the dislocation loops [14]. Although we do not have any direct evidence for the increased dislocation loop density, more defects should soften the system so that the large focal conic domains are not strongly penalized by their elastic energy. Therefore the rapid growth of the focal conic domain size close to the transition temperature may reflect the proliferation of dislocation loops as predicted by the theory [12,23].

When the shear rate is increased at constant temperature as in figs. 4(d)–(f), on the other hand, we clearly see that the width of oily streak decreases systematically. This tendency is also consistent with the prediction that the size of focal domains L is a decreasing function of $\dot\gamma$ in Regime I, or more precisely, a power law behavior $L \sim \dot\gamma^{-1/5}$ as discussed in refs. [8,9]. Although it is difficult to confirm this relation quantitatively from the microscope observation, we find that the defect density increases for higher shear rates. This phenomena reflects the

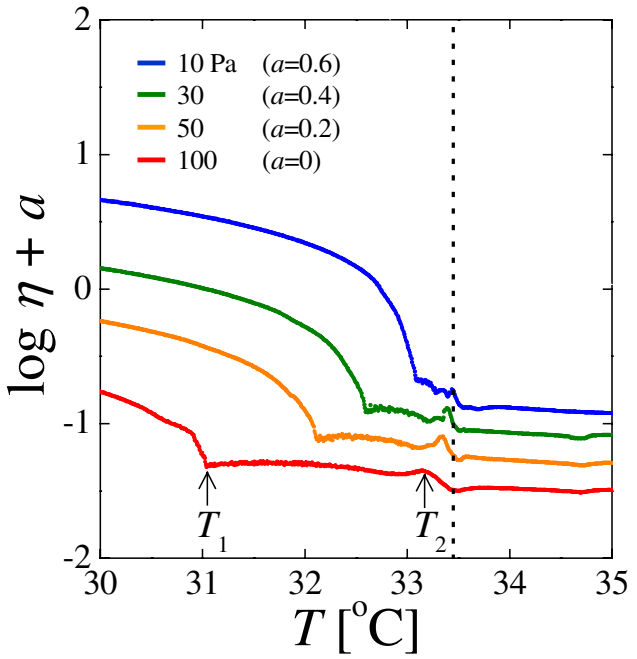

Fig. 5: (Colour on-line) Shear viscosity η as a function of the temperature obtained at different applied shear stress $\sigma = 10$, 30, 50, 100 Pa. Here $\log \eta$ is shifted by a constant a in order to have a better visibility. Vertical dotted line indicates $T = T_{\rm SN}$.

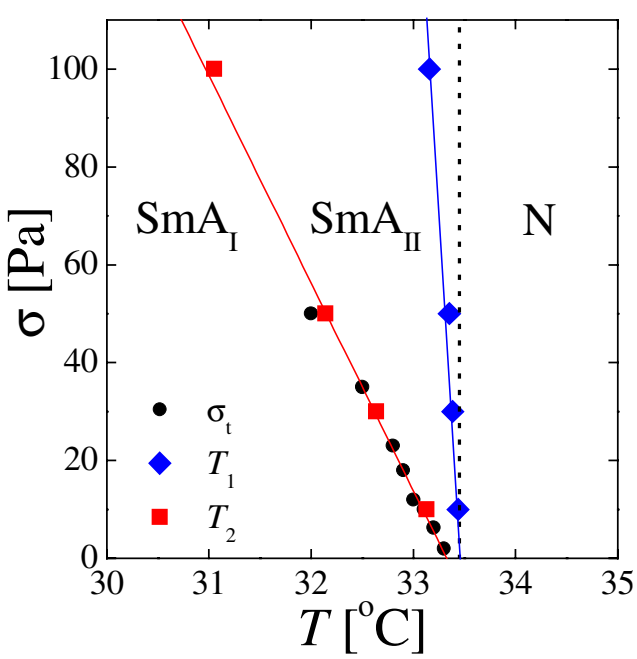

Fig. 6: (Colour on-line) Dynamic phase diagram of 8CB under shear plotted against the temperature and the applied shear stress σ. $\sigma_{\rm t}$ is the stress above which the smectic becomes Newtonian in fig. 1, while T_1 and T_2 are characteristic temperatures identified in fig. 5. The vertical dotted line indicates $T = T_{\rm SN}$. The lines of $\sigma_{\rm t}$ and T_1 coincide with each other. $\rm SmA_I$ and $\rm SmA_{II}$ denote the smectic phases in Regime I and II, respectively, while N indicates the nematic phase.

proliferation of dislocation loops due to the non-equilibrium shear flow. In Regime II, we could not observe oily streaks at high shear rate where the Newtonian behavior appeared.

Dynamic phase diagram. In addition to the existing dislocations in thermal equilibrium, those induced by shear flow might also affect the rheological properties of the smectic phase. In order to construct a dynamic phase diagram, we have measured the temperature dependence of the shear viscosity η under different applied shear stresses 10, 30, 50 and 100 Pa. The result is shown in fig. 5 in which η showed a rather complicated temperature dependence. In the low temperatures, the viscosity decreased by increasing the temperature, followed by a plateau region starting at T_1. A further increase in the temperature caused a peak at T_2 slightly below $T_{\rm SN}$. Interestingly, both T_1 and T_2 shifted to lower temperatures as the applied shear stress is increased.

In fig. 6, the two characteristic temperatures T_1 and T_2 are plotted against the applied shear stress σ together with the data of $\sigma_{\rm t}$ at which the transition from Regime I to Regime II takes place (as determined in fig. 1). In this plot, we see that T_1 and T_2 varies linearly with σ, and so does $\sigma_{\rm t}$. More importantly, the data of T_1 and $\sigma_{\rm t}$ coincide with each other. The extrapolations of T_1 and T_2 to zero shear stress give a temperature which is in accord with $T_{\rm SN}$ at the quiescent state. In the lower-temperature region, $T < T_1$, where the viscosity exhibited a remarkable temperature dependence, the smectic is shear thinning (Regime I) and is denoted as $\rm SmA_I$. In the intermediate-temperature region, $T_1 < T < T_2$, where the viscosity is almost constant, the smectic is Newtonian (Regime II) and is denoted as $\rm SmA_{II}$. These regions are marked in fig. 6.

This rheological transition from the shear thinning ($\rm SmA_I$) to the Newtonian behavior ($\rm SmA_{II}$) can be compared with fig. 11 in ref. [17]. In their case, the orientation diagram of the smectic phase consists of two regimes: i) the shear thinning regime ($m = 2$) where a leek structure is oriented along the flow direction, ii) the Newtonian regime ($m = 1$) where the perpendicular orientation of layers is observed. Our result is almost in accord with these behaviors, although the line separating between these two regimes slightly deviates from our data of T_1 or $\sigma_{\rm t}$. As a consequence, the temperature at which the $\rm SmA_I$ phase disappears in their case do not coincide with $T_{\rm SN}$, and is about 1.6 °C higher. Although the system presented a hysteresis in ref. [17], we did not observe any apparent discontinuous jump in the shear rate when the transition from $\rm SmA_I$ to $\rm SmA_{II}$ takes place. Our phase diagram is also consistent with the orientation transition discussed by Safinya *et al.* [15]. In the $\rm SmA_{II}$ regime, they observed the perpendicular orientation where the layer normal points along the vorticity direction. Since a cybotactic cluster encourages the layer fluctuation around the SmA-N transition [23], a scattering pattern, as observed by Panizza *et al.*, suggests that the perpendicular orientation is attributed to the cybotactic cluster.

Apart from the rheological transition in the smectic phase, the applied shear stress dependence of T_2 in figs. 5 and 6 implies a non-equilibrium structural transition to the nematic phase under shear flow. The decrease in T_2 in the presence of the applied shear stress strongly indicates the shear-induced melting of the smectic order. This is because the proliferation of the dislocation loop is caused both by the equilibrium temperature close to the transition point and by the non-equilibrium shear flow. In the nematic phase, the flow behavior is completely Newtonian, and cannot be distinguished from the SmA_{II} phase from the rheological point of view. The transition to the nematic phase under flow was also confirmed by the microscope observation (not presented here) in which we see the appearance of disclination lines instead of dislocations. Although we have observed the lowering of the transition temperature, Safinya *et al.* reported an opposite tendency when the transition temperature was approached from above, *i.e.*, from the nematic phase [15,16].

Conclusion. – To conclude, we have investigated the rheological properties of a thermotropic liquid crystal 8CB in the smectic phase close to the Sm-N transition temperature. For each flow curve at different temperatures, three different regimes were identified depending on the applied shear stress: i) appearance of the yield stress at low stresses (Regime 0), ii) power law behavior at intermediate shear stresses (Regime I), and iii) Newtonian at higher shear stresses (Regime II). The fact that the yield stress vanishes at the Sm-N transition temperature is due to the rapid increment of the focal conic domain size, which may reflect the unbinding behavior of dislocation loops. The constructed dynamic phase diagram exhibits two different smectic phases (SmA_I and SmA_{II}), in agreement with the previous experimental results. We also found that the applied shear stress decreases the Sm-N transition temperature.

* * *

We acknowledge useful discussions with H. Orihara. We thank T. Takahashi and M. Imai for allowing us to use the rheometer MCR-300 and the Linkam shear cell CSS-450, respectively. SF and SK acknowledge support by KAKENHI (Grant-in-Aid for Scientific Research) on Priority Areas "Soft Matter Physics" and Grant No. 21540420 from the Ministry of Education, Culture, Sports, Science and Technology of Japan.

REFERENCES

[1] Larson R. G., *The Structure and Rheology of Complex Fluids* (Oxford University Press, Oxford) 1999.
[2] Oswald P. and Pieranski P., *Smectic and Columner Liquid Crystals* (Taylor & Francis, Boca Raton) 2006.
[3] Larson R. G., Winey K. I., Patel S. S., Watanabe H. and Bruinsma R., *Rheol. Acta*, **32** (1993) 245.
[4] Horn R. G. and Kleman M., *Ann. Phys. (N.Y.)*, **3** (1978) 229.
[5] Colby R. H., Ober C. K., Gillmor J. R., Connelly R. W., Duong T., Galli G. and Laus M., *Rheol. Acta*, **36** (1997) 498.
[6] Colby R. H., Nentwich L. M., Clingman S. R. and Ober C. K., *Europhys. Lett.*, **54** (2001) 269.
[7] Moller P. C. F., Mewis J. and Bonn D., *Soft Matter*, **2** (2006) 274.
[8] Meyer C., Asnacios S., Bourgaux C. and Kleman M., *Rheol. Acta*, **39** (2000) 223.
[9] Meyer C., Asnacios S. and Kleman M., *Eur. Phys. J. E*, **6** (2001) 245.
[10] Orowan E., *Proc. Phys. Soc. (London)*, **52** (1940) 8.
[11] Lu C.-Y. D., Chen P., Ishii Y., Komura S. and Kato T., *Eur. Phys. J. E*, **25** (2008) 91.
[12] Helfrich W., *J. Phys. (Paris)*, **39** (1978) 1199.
[13] Nelson D. R. and Toner J., *Phys. Rev. B*, **24** (1981) 363.
[14] Moreau P., Navailles L., Giermanska-Kahn J., Mondain-Monval O., Nallet F. and Roux D., *Europhys. Lett.*, **73** (2006) 49.
[15] Safinya C. R., Sirota E. B. and Plano R. J., *Phys. Rev. Lett.*, **66** (1991) 1986.
[16] Bruinsma R. F. and Safinya. C. R., *Phys. Rev. A*, **43** (1991) 5377.
[17] Panizza P., Archambault P. and Roux D., *J. Phys. II*, **5** (1995) 303.
[18] Bandyopadhyay R., Liang D., Colby R. H., Harden J. L. and Leheny R. L., *Phys. Rev. Lett.*, **94** (2005) 107801.
[19] Sollich P., Lequeux F., Hébraud P. and Cates M. E., *Phys. Rev. Lett.*, **78** (1997) 2020.
[20] Basappa G., Suneel , Kumaran V., Nott P. R., Ramaswamy S., Naik V. M. and Rout D., *Eur. Phys. J. B*, **12** (1999) 269.
[21] Dehz O., Nallet F. and Diat O., *Europhys. Lett.*, **55** (2001) 821.
[22] Goulian M. and Milner S. T., *Phys. Rev. Lett.*, **74** (1995) 1775.
[23] de Gennes P. G. and Prost J., *The Physics of Liquid Crystals* (Carendon Press, London) 1993.
[24] Zywocinski A., Picano F., Oswald P. and Geminard J. C., *Phys. Rev. E*, **62** (2000) 8133.